Available online at www.sciencedirect.com

ScienceDirect

Polymer 49 (2008) 1049–1055

polymer

www.elsevier.com/locate/polymer

Investigation on interfacial interaction of flame retarded and glass fiber reinforced PA66 composites by IGC/DSC/SEM

Xiaohua Huang, Bin Li*, Baoli Shi, Liping Li

Heilongjiang Key Laboratory of Molecular Design and Preparation of Flame Retarded Materials,
College of Science, Northeast Forestry University, Harbin, Heilongjiang 150040, PR China

Received 1 May 2007; received in revised form 13 November 2007; accepted 23 December 2007
Available online 5 January 2008

Abstract

The interfacial interaction of flame retarded and glass fiber reinforced PA66 composites is a very important issue due to one of the key factors influencing the mechanical properties of materials. In this article, the interfacial interaction among the components in the composites has been studied by IGC/DSC/SEM techniques. The experimental data demonstrated that Zn^{2+}-modified melamine polyphosphate (Zn–MpolyP) flame retardant could obviously enhanced the mechanical properties of the composites compared with melamine polyphosphate (MpolyP). SEM results proved that Zn–MpolyP could well disperse in the composites, and effectively improve the interfacial compatibility of the composites. Based on DSC results, Zn–MpolyP and MpolyP promoted the crystallization enthalpy (ΔH_c) and temperature (T_c) of PA66 to increase. Zn–MpolyP showed more effect in increasing the crystallization degree of PA66 than MpolyP. They exhibited the nucleating effect in PA66. The Lewis acid–base numbers (K_a and K_b) and their ratio (K_b/K_a) obtained by inverse gas chromatography (IGC) further proved that the strongest Lewis acid–base interaction between PA66 and Zn–MpolyP existed in the composites. This result is probably due to the strong complex between Zn^{2+} in Zn–MpolyP and lone pair electrons at O and N atoms of PA66 and glass fiber. Therefore, the all results of IGC/DSC/SEM techniques demonstrated that the interfacial compatibility of components in composites was better improved by Zn–MpolyP than MpolyP.

Keywords: Composite; Interfacial interaction; Flame retardant

1. Introduction

Polyamide materials are semicrystalline engineering plastics used for numerous engineering applications due to good chemical resistance, high tensile and flexural strengths, good abrasion, and easy processing performance [1–8]. In order to further obtain high impact strength, good dimension stability, high modulus and low water absorption, the glass fiber reinforced polyamide composites have been widely emphasized. They have been widely applied in Electronic and Electric (E&E) applications. However, many applications of glass fiber reinforced polyamide composites are restricted because of their easy flammability. Most researchers [8–10] have been paying attention to Research and Development (R&D) of the flame retarded and glass fiber reinforced polyamide composites, especially polyamide 66 (PA66) and polyamide 6 (PA6).

Due to the black smoke and erosive gases that halogen containing flame retardant polymeric materials produce during burning [11,12], halogen-free flame retardancy has become a hot point in flame retardant researches [10,13–19]. Many researches have proved that melamine cyanurate is an effective flame retardant for PA66 and PA6 [20], however, it presents a low flame retardancy in the glass fiber reinforced PA66 and PA6 systems due to the ‘‘candlewick effect’’ of glass fiber. Microcapsule red phosphorus can be used in glass fiber reinforced polyamide composites, and shows good flame retardancy, however, its application is limited due to red color and phosphine produced at the processing. Melamine polyphosphate

---

* Corresponding author. Tel./fax: +86 451 8219 1571.
E-mail address: libinzh62@163.com (B. Li).

0032-3861/$ - see front matter © 2008 Elsevier Ltd. All rights reserved.
doi:10.1016/j.polymer.2007.12.037

(MpolyP) has been proved to be a very important and effective flame retardant for glass fiber reinforced PA66 and PA6 [3], of which the flame retardancy can reach UL-94 V-0 rating. Jahromi and co-workers [21] reported the effect of MpolyP on thermal degradation mechanism of PA66 and PA6. In our recent research work, Zn^{2+}-modified MpolyP flame retardant synthesized in our laboratory was applied in glass fiber reinforced PA66 composites [22,23].

As all we know, the surface and interface properties are important factors influencing mechanical properties of materials [24]. Kazuya and co-workers [25] reported the aggregation structure and molecular motion on interface in glass fiber reinforced PA66 composites. But the reports on the interface interaction of flame retarded and glass fiber reinforced PA66 are few at present.

Inverse gas chromatography (IGC) is a characterization technique for surface properties of solid materials [26−29]. Lewis acid−base numbers (K_a and K_b) obtained by IGC have been used to explain the interfacial interaction between materials [24]. This contribution is aimed to gain a better understanding of the interfacial interaction among PA66, glass fiber and flame retardants by the combination of inverse gas chromatography (IGC), differential scanning calorimetry (DSC) and scanning electron microscopy (SEM).

2. Experimental

2.1. Materials

PA66 (101L) used in this work was purchased from Dupont Ltd., USA. Glass fibers were purchased from Jushi group Co., Ltd., China. The flame retardants of Zn−MpolyP and MpolyP were synthesized in our laboratory.

For the IGC analysis, the apolar *n*-alkane probes were *n*-hexane (C_6), *n*-heptane (C_7), and *n*-octane (C_8), *n*-nonane (C_9) and *n*-decane (C_{10}). Dichloromethane (CH_2Cl_2), trichloromethane ($CHCl_3$), acetone (Acet), ether and tetrahydrofuran (THF) were used as the polar probes, and *n*-pentane was used as the reference probe. All probes were of analytical grade, and were purchased from Tianjin Kermel Chemical Reagents Development Center, China. The surface characteristics of the probes [29−34] are listed in Table 1.

Table 1
Characteristics of the probe solvents

Probes	a (Å^2)	r_1^d (mJ/m^2)	$a(r_1^d)^{0.5}$ (Å^2 (mJ/m^2)$^{0.5}$)	AN* (kJ/mol)	DN (kJ/mol)
n-C_6	51.5	18.4	221		
n-C_7	57.0	20.3	257		
n-C_8	63.0	21.3	291		
n-C_9	69.0	22.6	329		
n-C_{10}	75.0	23.4	363		
CH_2Cl_2	31.5	27.6	165	16.3	0.0
$CHCl_3$	44.0	25.9	224	22.7	0.0
Acet	42.5	16.5	173	10.5	71.4
Ether	47.0	15.0	182	5.88	80.6
THF	45.0	22.5	213	2.10	84.4

Chromosorb 101 (80−100 mesh) purchased from Shanghai Chemical Plant of China was used as the column stationary phase support for PA66.

2.2. Composite preparation

The formulations of the composites mainly included PA66, glass fiber, and flame retardants (MpolyP and Zn−MpolyP). The glass fiber was fixed at 25 wt% in the composites, and the loadings of PA66 and the flame retardants were 75, 70, 65, 60, 55, 50 wt% and 0, 5, 10, 15, 20, 25 wt%, respectively. In order to improve the processing performance, polysiloxane, as a processing aid, was used in the formulations, and its loading was 0.7 wt% based on the total formulation mass. These formulations were extruded by using a co-rotating 35-mm twin-screw extruder (TE-35, Nanjing Jieya Extruder Equipment Co., Ltd., China) at the operating temperatures of 270−275 °C, and then cut into granules. Finally, the granules were injected to form sample bars for testing impact strength, tensile strength and flexural strength, using an injection molding machine (HTF86X1-A, HaiTian Groups, China) at the injection temperature of 280−290 °C.

2.3. Inverse gas chromatography

The inverse gas chromatography (IGC) measurements were carried out on an Agilent 6850 gas chromatograph instrument equipped with a flame ionization detection (FID) system. Pure nitrogen was used as the carrier gas. The column temperature ranges, the sample weights and the flow rates are listed in Table 2. The temperature of injector and FID was set to 130 °C. The probe solvents were manually injected into the column by a 1.0 μL Hamilton syringe. The injection volumes were 0.1 μL. The column was a stainless steel tube (0.5 m length, 4.24 mm i.d.), washed with acetone prior to use. PA66 coated on chromosorb 101, glass fiber, Zn−MpolyP and MpolyP was filled in the stainless column. K_a and K_b of each material were calculated according to the net retention volume obtained from IGC.

2.4. DSC

Differential scanning calorimetry tests were carried out on Perkin−Elmer Diamond DSC. The weight of each sample was ranged from 4 mg to 5 mg. All samples were heated from the room temperature to 280 °C at a heating rate of 150 °C/min, then kept at this temperature for 5 min to release all stresses and the thermal history. Finally, the samples were then cooled from 280 °C to 25 °C at a constant rate of 10 °C/min. The

Table 2
IGC experimental conditions

Materials	Temperature range (K)	Temperature increment (K)	Flow rate (cm^3/min)	Sample weight (g)
PA66	343.3−373.3	10	10.5	0.2287
Glass fiber	343.3−373.3	10	7.0	2.0995
Zn−MpolyP	373.3−403.3	10	20.0	0.5893
MpolyP	373.3−403.3	10	20.0	1.0261

crystallization enthalpy (ΔH_c) and crystallization temperature (T_c) of PA66 were obtained by calculating.

2.5. Mechanical property tests

Tensile strength, flexural strength and Izod impact of all samples were obtained on a Regeer computer controlled mechanical instrument and Notched Izod impact instrument, respectively, according to the ASTM standards.

2.6. SEM

The fractured surfaces of the composites obtained under the liquid nitrogen condition were coated with gold to prevent electrical charging. The surface morphological images of all samples were observed by the FEI Quan Ta200 SEM of Holland at an acceleration voltage of 15 kV.

3. Results and discussion

3.1. Mechanical properties

MpolyP and Zn–MpolyP, as flame retardants, were used in glass fiber reinforced PA66 systems to obtain the flame retardant composites because they are considered to be very effective in the flame retardancy, and UL-94 V-0 rating of the composites are achieved when the loading of the flame retardants were kept at 25 wt%.

Figs. 1–3 show the influence of flame retardants on the tensile strength, flexural strength and Notched Izod impact strength of the flame retarded and glass fiber reinforced PA66 composites, respectively. From Figs. 1–3, it is observed that tensile strength and flexural strength of the PA66 composites increased with the increase of flame retardants, while Notched Izod impact strength decreased compared with the glass fiber reinforced PA66. When the addition of the flame retardant reached about 15 wt%, mechanical properties of the composites presented the best values. It is deserved to mention that Zn–MpolyP exhibited much more excellent mechanical properties compared with MpolyP in the composites. This result indicated that Zn^{2+} in Zn–MpolyP probably presents more interfacial function among PA66, Zn–MpolyP and glass fiber, which has been proved in the following sections. However, at the higher loading, the flame retardant mechanical properties of the composites presented the decreasing tendency. Figs. 4 and 5 show the tensile strength and flexural strength of net PA66 curves versus the loading of the flame retardants. It is observed that Zn–MpolyP and MpolyP showed different influence on the mechanical properties of net PA66. Zn–MpolyP is more beneficial to obtain better tensile strength and flexural strength of net PA66 compared to MpolyP. This tendency is in agreement with that of the glass fiber reinforced PA66 system. Furthermore, the influence of flame retardants

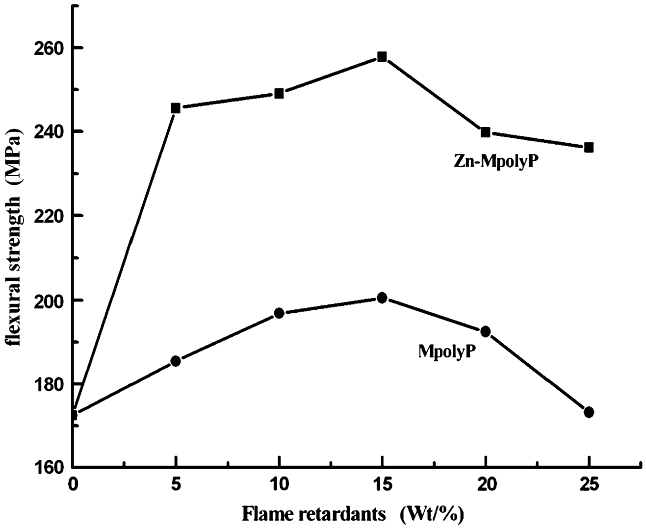

Fig. 2. Effect of flame retardants on flexural strength of glass fiber reinforced flame retarded PA66.

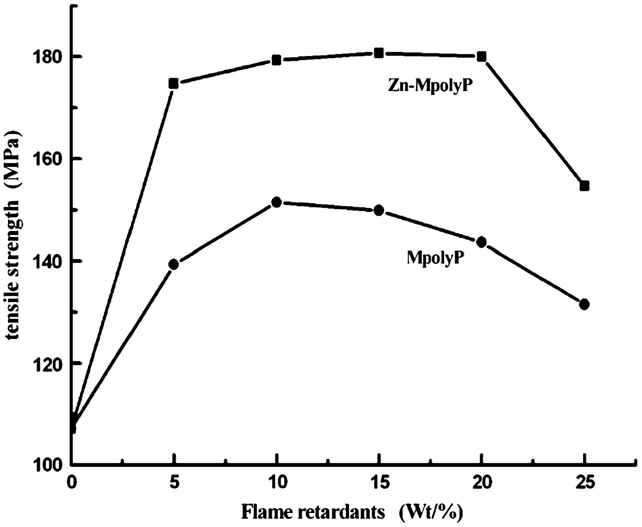

Fig. 1. Effect of flame retardants on tensile strength of glass fiber reinforced flame retarded PA66.

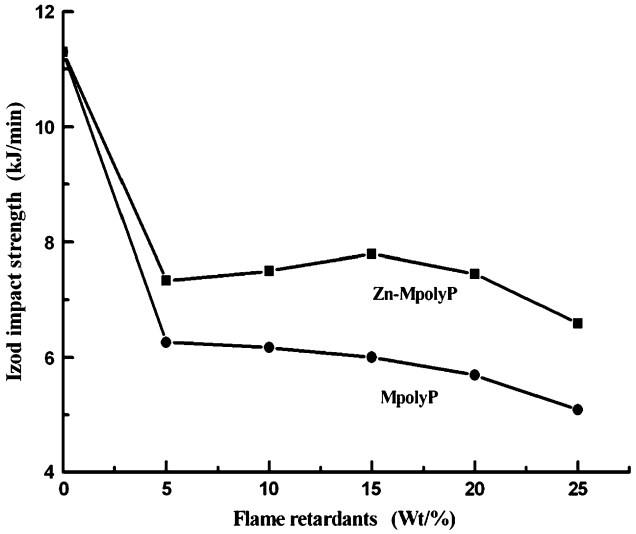

Fig. 3. Effect of flame retardants on Notched Izod impact of glass fiber reinforced flame retarded PA66.

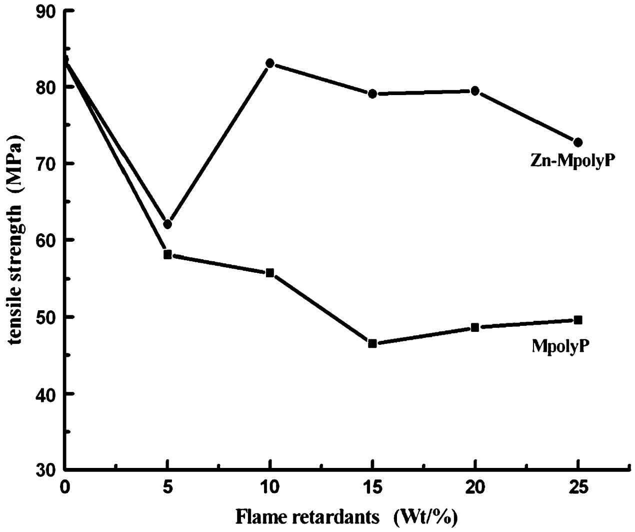

Fig. 4. Effect of flame retardants on tensile strength of PA66.

on Notched Izod impact strength of net PA66 is not given in this contribution because their values including net PA66 were low and kept at between 1.8 kJ/m^2 and 3.2 kJ/m^2.

3.2. Morphological structures of the PA66 composites by SEM

Figs. 6–8 show the images of the glass fiber reinforced PA66 and the flame retarded and glass fiber reinforced PA66 composites with 25 wt% loading of flame retardants. In Fig. 6, the surface of glass fibers was smooth, and glass fibers were easily pulled out from PA66 matrix. This fact indicated that the interfacial interaction between PA66 and glass fiber was not good. However, from Figs. 7 and 8, the flame retardants, such as MpolyP and Zn–MpolyP, were well dispersed in the glass fiber reinforced PA66 composites, and obviously improved the interfacial interaction between glass fibers and PA66 composites. The toughness and strength of the composite matrix treated with Zn–MpolyP were much better than those of the composite matrix treated with MpolyP based upon SEM images (see Figs. 7 and 8), which has been proved by the mechanical properties of the composites.

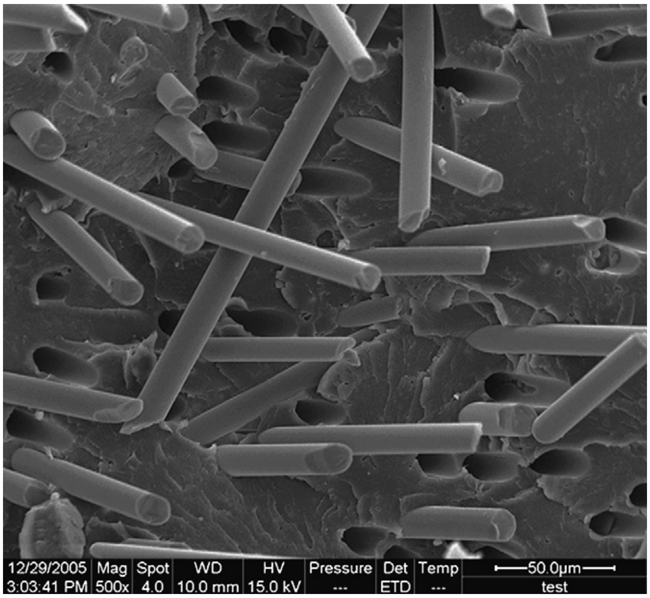

Fig. 6. SEM image of glass fiber reinforced PA66.

3.3. Crystallization behavior of the PA66 composites by DSC

Figs. 9 and 10 show the variation of the enthalpy (ΔH_c) and temperature (T_c) of PA66 crystallization versus the loadings of the flame retardants. From Figs. 9 and 10, MpolyP and Zn–MpolyP could clearly enhance the enthalpy of PA66 crystallization in the composites, Zn–MpolyP presented the better prominence, and they obviously enhanced T_c. These results demonstrated that

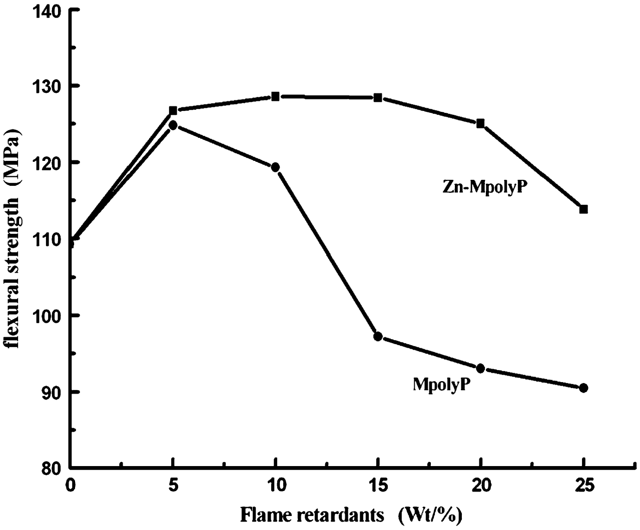

Fig. 5. Effect of flame retardants on flexural strength of PA66.

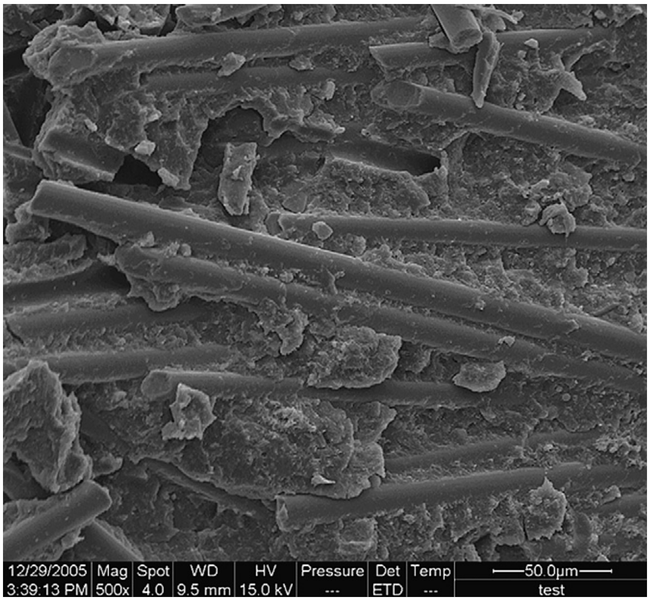

Fig. 7. SEM image of glass fiber reinforced MpolyP flame retarded PA66.

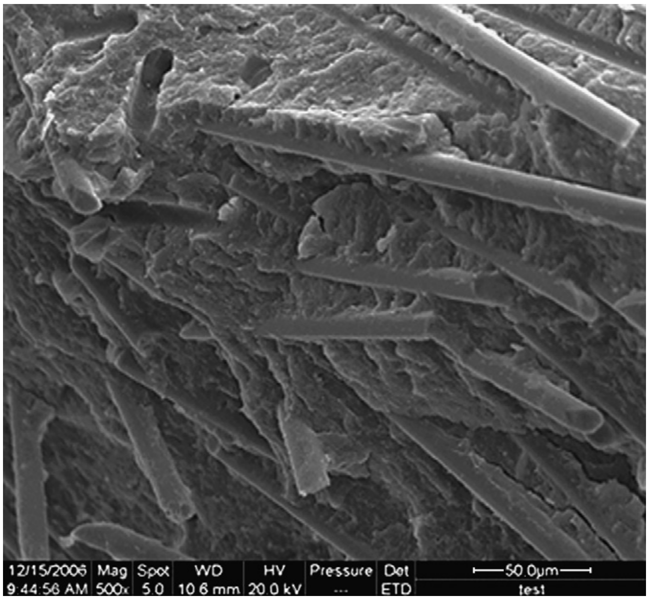

Fig. 8. SEM image of glass fiber reinforced Zn–MpolyP flame retarded PA66.

MpolyP and Zn–MpolyP promoted the crystallization of PA66 and enhanced the crystallization degree of PA66, and Zn–MpolyP was more effective than MpolyP. This is because they present the good nucleation function in PA66, which of MpolyP has been proved in our recent research [3]. Therefore, increasing the crystallization degree is one of the reasons enhancing the mechanical properties of the composites. However, ΔH_c of PA66 crystallization gradually decreased with the increase of the flame retardants based on Fig. 9. This indicated that the increase of the flame retardants in the composites should lower the mechanical properties, whereas the mechanical properties of the composites increased at the loading of flame retardants between 5 wt% and 15 wt%. These results further proved that the flame retardants, especially Zn–MpolyP, could simultaneously promote the crystallization of PA66 and improve the interfacial interaction among components in the composites.

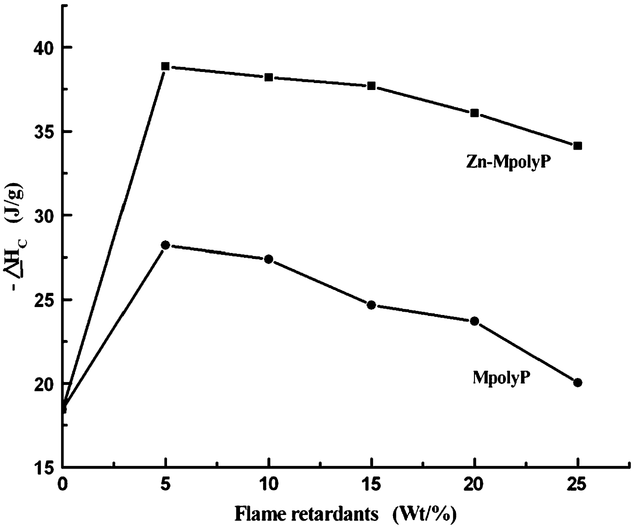

Fig. 9. Effect of flame retardants on the enthalpy of crystallization.

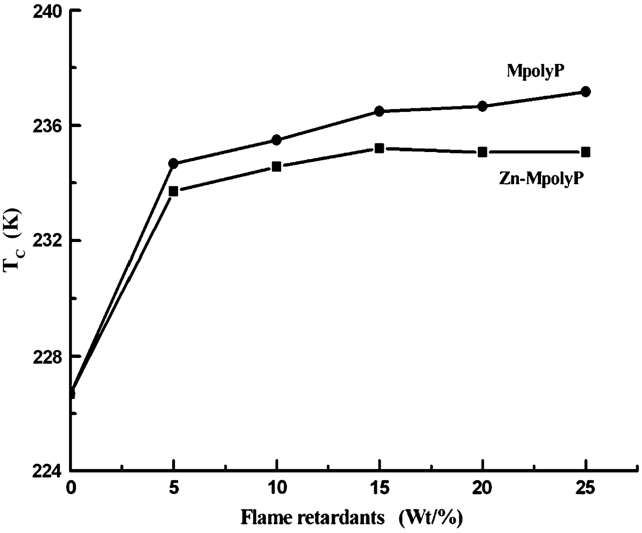

Fig. 10. Effect of flame retardants on crystallization temperature.

3.4. Lewis acid–base numbers K_a and K_b of the components in the PA66 composites by IGC

Surface Lewis acid–base properties of materials are very significant, which have been applied to explain the interfacial interaction between materials [24]. Lewis acid–base numbers, K_a and K_b, can be easily obtained by IGC technique [26,35–37]. Fig. 11 shows the plots of $RT\ln(V_n)$ versus $a(r_1^d)^{0.5}$ for n-alkanes at the given temperature based on Eq. (1) [30,38]. Fig. 11 only gives an example for PA66, the plots of other materials including glass fiber, Zn–MpolyP and MpolyP are similar to Fig. 11, which are omitted in the contribution. The similar treatment is followed in Fig. 12

$$-\Delta G_a = RT\ln(V_n) = 2N_A a\left(\gamma_s^d\right)^{0.5}\left(\gamma_l^d\right)^{0.5} + K' \quad (1)$$

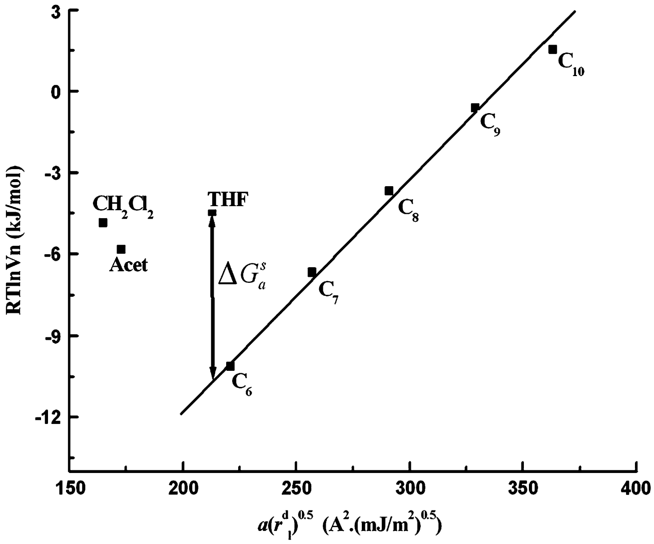

Fig. 11. Free energy of adsorption for PA66 versus $a(r_1^d)^{0.5}$ for n-alkanes and polar probes.

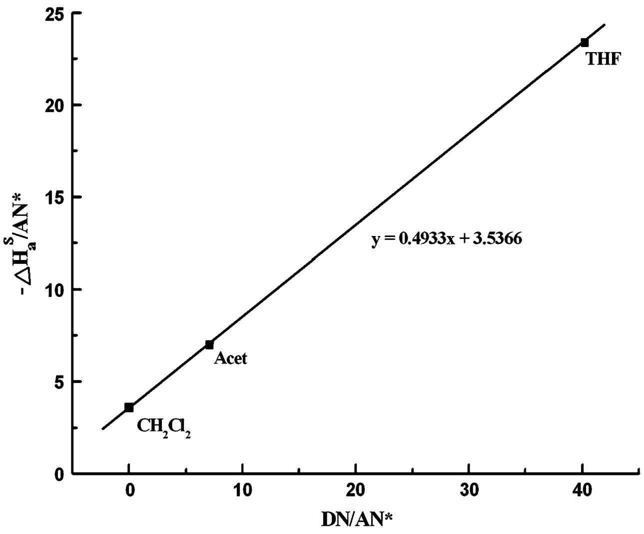

Fig. 12. Determination of K_a and K_b for the surface Lewis acid–base of PA66.

From Fig. 11, all curves showed the good linear relationship. The free energy of adsorption by Lewis acid–base interactions (ΔG_a^s) for the polar probes was calculated based on the data shown in Fig. 11 and Eq. (2) [30,39]. All the data of ΔG_a^s were obtained at the overall temperature points and are listed in Table 3.

According to Eq. (3), the enthalpy of Lewis acid–base interactions (ΔH_a^s) for every polar probe was calculated from the ΔG_a^s listed in Table 3. The calculated results are listed in Table 4. Based on the data of ΔH_a^s and Eq. (4), the plots of $-\Delta H_a^s/\text{AN}^*$ versus DN/AN* for the polar probes shown in Fig. 12 were used to calculate Lewis acid–base parameters, K_a and K_b. All the data of K_a and K_b for every material are listed in Table 5.

$$\Delta G_a = \Delta G_a^d + \Delta G_a^s \tag{2}$$

Table 4
Enthalpy of Lewis acid–base interactions of materials for different probes

Materials	Enthalpy of Lewis acid–base interactions, ΔH_a^s (kJ/mol), for different probes				
	CH_2Cl_2	$CHCl_3$	Acet	THF	Ether
PA66	58.71	–	70.24	49.08	–
Glass fibers	–	−55.88	−70.24	−49.08	–
Zn–MpolyP	–	−43.43	−36.29	−39.88	−37.19
MpolyP	–	−31.12	−21.21	−22.65	−25.79

Table 5
Lewis acid–base numbers (K_a and K_b) of the materials

Materials	K_a	K_b	K_b/K_a
PA66	0.49	3.54	7.17
Glass fiber	0.51	2.86	5.61
Zn–MpolyP	0.44	1.02	2.32
MpolyP	0.24	0.96	4.00

$$\Delta G_a^s = \Delta H_a^s - T\Delta S_a^s \tag{3}$$

$$-\Delta H_a^s = K_a \times \text{DN} + K_b \times \text{AN}^* \tag{4}$$

Based on K_b values summarized in Table 5 all the materials are basic, and PA66 showed the strongest Lewis base, while Zn–MpolyP presented the weakest Lewis base. The ratio of K_b to K_a (K_b/K_a) was used to represent the relative strength of Lewis base–acid due to different values of K_b and K_a of materials [40–43]. The higher the relative strength of Lewis base–acid (K_b/K_a) is, the stronger the basicity of the material is, otherwise, the weaker the acidity of the material is. Therefore, there were very strong Lewis acid–base interaction between PA66 and Zn–MpolyP or MpolyP, especially, the Lewis acid–base interaction between PA66 and Zn–MpolyP was stronger than that between PA66 and MpolyP, and the Lewis acid–base interaction between glass fiber and Zn–MpolyP was stronger than that between glass fiber and MpolyP. This further proved that Zn–MpolyP can more effectively improve

Table 3
Free energy of adsorption by Lewis acid–base interactions

Materials	Polar probe	Free energy of adsorption, ΔG_a^s (kJ/mol), at different temperatures						
		343.2 (K)	353.2 (K)	363.2 (K)	73.3 (K)	383.2 (K)	393.2 (K)	403.2 (K)
PA66	CH_2Cl_2	5.12	7.08	9.54	10.50	–	–	–
	Acet	3.60	5.66	7.91	10.04	–	–	–
	THF	3.07	4.49	6.01	7.65	–	–	–
Glass fiber	CH_2Cl_2	5.12	7.08	9.54	10.50	–	–	–
	Acet	3.60	5.66	7.91	10.04	–	–	–
	THF	3.07	4.49	6.01	7.65	–	–	–
Zn–MpolyP	Acet	–	–	–	0.022	0.024	0.027	0.029
	$CHCl_3$	–	–	–	0.003	0.009	0.012	0.014
	THF	–	–	–	0.012	0.015	0.018	0.020
	Ether	–	–	–	0.018	0.021	0.023	0.026
MpolyP	Acet	–	–	–	7.48	8.25	9.07	9.77
	$CHCl_3$	–	–	–	1.34	2.13	3.10	3.92
	THF	–	–	–	4.03	4.67	5.39	6.17
	Ether	–	–	–	5.69	6.47	7.35	8.21

the interfacial interaction of the composites. This result is in agreement with that of SEM. This is probably due to the strong complex between Zn^{2+} in Zn−MpolyP and lone pair electrons at O and N atoms of PA66 and glass fiber.

4. Conclusions

Mechanical properties and interfacial interaction of glass fiber reinforced PA66 composites treated with MpolyP or Zn−MpolyP were investigated. Mechanical properties, such as tensile strength and flexural strength, were enhanced by MpolyP and Zn−MpolyP compared with the glass fiber reinforced PA66 composite. Zn−MpolyP presented the best mechanical properties of the composites than MpolyP. These results are attributed to the good interfacial interaction among the components in the composites, which has been proved by IGC/DSC/SEM techniques. DSC results indicated that Zn−MpolyP, as a nucleating agent, could clearly increase the crystallization degree and temperature of PA66, and SEM results showed the improvement of the interfacial interaction among components in the composites. IGC results proved that the strongest Lewis acid−base interaction between Zn−MpolyP and PA66 was presented due to the highest K_b/K_a value of PA66 and the lowest K_b/K_a value of Zn−MpolyP.

Acknowledgements

This work was supported by Heilongjiang Key Project Technologies R&D Programme (Number: GB03A203), Heilongjiang Science fund for Distinguished Young Scholar (Grant No.: JC04-06) and National Key Technology R&D Program (Grand No.: 2006BAE03B05).

References

[1] Zhang H, Zhang Z, Yang JL, Klaus F. Polymer 2006;47:679−89.
[2] Lin DJ, Chang CL, Lee CK, Cheng LP. Eur Polym J 2006;42:356−67.
[3] Li LP, Li B, Tang F. Eur Polym J 2007;43:2604−11.
[4] Seo Y, Kim B, Kim KU. Polymer 1999;40:4483−92.
[5] Chavarria F, Paul DR. Polymer 2004;45:8501−15.
[6] Averett RD, Realff ML, Michielsen S, Neu RW. Compos Sci Technol 2006;66(11):1671−81.
[7] Albano C, Sciamanna R, Gonzalez R, Papa J, Navarro O. Eur Polym J 2001;37:851−60.
[8] Chen YH, Wang Q. Polym Degrad Stab 2006;91:2003−13.
[9] Jou WS, Chen KN, Chao DY, Lind CY, Yehd JT. Polym Degrad Stab 2001;74:239−45.
[10] Liu Y, Wang Q. Polym Degrad Stab 2006;91:3103−9.
[11] Bhaskar T, Kaneko J, Muto A, Sakata Y, Jakab E, Matsui T, et al. J Anal Appl Pyrolysis 2004;71:765−77.
[12] Uddin MA, Bhaskar T, Kaneko J, Muto A, Sakata Y, Matsui T. Fuel 2002;81:1819−25.
[13] Liu Y, Wang Q, Fei GX, Chen YH. J Appl Polym Sci 2006;102: 1773−9.
[14] Modesti M, Lorenzetti A. Polym Degrad Stab 2002;78:167−73.
[15] Becker L, Lenoir D, Matuschek G, Kettrup A. J Anal Appl Pyrolysis 2001;60:55−67.
[16] Gao F, Tong LF, Fang ZP. Polym Degrad Stab 2006;91:1295−9.
[17] Du LC, Qu BJ, Xu ZJ. Polym Degrad Stab 2006;91:995−1001.
[18] Qin HL, Zhang SM, Zhao CG, Hu GJ, Yang MS. Polymer 2005;46: 8386−95.
[19] Perez RM, Sandler JKW, Altstadt V, Hoffmann T, Pospiech D, Ciesielski M, et al. Polymer 2007;48:778−90.
[20] Gijsman P, Steenbakkers R, Furst C, Kersjes J. Polym Degrad Stab 2002;78:219−24.
[21] Jahromi S, Gabrielse W, Braam A. Polymer 2003;44:25−37.
[22] Li B, Tang F, Sun CY, Li XL. Chinese patent 200510010255.7; 2005.
[23] Li B, Li LP, Huang XH, Tang F. Chinese patent 200610150960.1; 2006.
[24] Santos JMRCA, Fagelman K, Guthrie JT. J Chromatogr A 2002;969: 119−32.
[25] Kazuya N, Michihiro T, Atsushi T, Tisato K. Polymer 2002;43:4055−62.
[26] Shi BL, Zhang QR, Jia LN, Liu Y, Li B. J Chromatogr A 2007;1149:390−3.
[27] Cava D, Gavara R, Lagaron JM, Voelkel A. J Chromatogr A 2007;1148: 86−91.
[28] Calhoun AA, Nicholson PD, Barnes AB. Polym Degrad Stab 2006;91: 1964−71.
[29] Perruchot C, Chehimi MM, Vaulay MJ, Benzarti K. Cem Concr Res 2006;36:305−19.
[30] Santos JMRCA, Guthrie JT. Mater Sci Eng R 2005;50:79−107.
[31] Hamieh T, Schultz J. J Chromatogr A 2002;969:17−25.
[32] Jandura P, Riedl B, Kokta BV. J Chromatogr A 2002;969:301−11.
[33] Kamdem DP. Langmuir 1993;9:3039−49.
[34] Hegedus CR, Kamel IL. J Coat Technol 1993;65:31−40.
[35] Shi BL, Zhao S, Jia LN, Wa LL. Carbohydr Polym 2007;67:398−402.
[36] Nastasovic AB, Onjia AE, Milonjic SK, Jovanovic SM. Eur Polym J 2005;41:1234−42.
[37] Santos JMRCA, Guthrie JT. J Chromatogr A 2005;1070:147−54.
[38] Santos JMRCA, Fagelman K, Guthrie JT. J Chromatogr A 2002;969: 111−8.
[39] Mukhopadhyay P, Schreiber HP. Colloids Surf A 1995;100:47−71.
[40] Abel ML, Chehimi MM, Fricker F, Delamar M. J Chromatogr A 2002;969:273−85.
[41] Uhlmann P, Schneider S. J Chromatogr A 2002;969:73−80.
[42] Dieckmann F, Klinger C, Uhlmann P, BoEhme F. Polymer 2001;42: 3463−6.
[43] Andrzejewska E, Voelkel A, Maga R, Andrzejewski M. Polymer 1998;39(15):3499−506.